



On the simultaneous estimation of model parameters used in constitutive laws for inelastic material behaviour

O.T. Bruhns,^{a,*} D.K. Anding^b

^a*Institute of Mechanics, Ruhr-University Bochum, D-44780 Bochum, Germany*

^b*Siemens AG, KWU G223S, D-45466 Mülheim/Ruhr, Germany*

Received in final revised form 30 August 1999

Abstract

The paper deals with the simultaneous estimation of parameters used in constitutive laws for modeling inelastic material behaviour. Experimental data is obtained from specimens with a uniform distribution of stresses. Uniaxial evaluations of the constitutive laws are used. Due to the numerical stiffness of the constitutive equations, it is shown that it is necessary to use an implicit time-integration scheme. The model parameters are estimated from experimental data using a least-squares criterion. Stochastic and deterministic optimization methods are used. The algorithms are parallelized on the basis of the master-slave paradigm. Since a complete parameter estimation requires error estimates and confidence regions, statistic methods are implemented. © 1999 Elsevier Science Ltd. All rights reserved.

Keywords: Inelasticity; Parameter identification; Stochastic and deterministic optimization methods; Inverse problem; Parallel computing; Sensitivity analysis

1. Introduction

Prediction of the behaviour of structures under mechanical and thermal loading requires accurate modelling of the material behaviour. For this purpose many models were developed in the past, which can be used in modern calculation methods like the Finite-Element-Method. Some of these models are introduced and explained in the books of Miller (1987), Ohtani et al. (1988), Lemaitre and Chaboche (1990) and Khan and Huang (1995).

* Corresponding author. Tel.: +49-234-700-3080; fax: +49-234-709-4229.

E-mail address: bruhns@tm.bi.ruhr.uni.bochum.de (O.T. Bruhns).

For an accurate modelling of the material behaviour a certain number of model parameters are necessary, depending on the model used. Models for the viscoplastic behaviour of materials (see also the works of Bodner and Partom, 1975; Chaboche and Rousselier, 1983; Krempl, 1987; Chaboche, 1989; Nouailhas, 1989; Schlums and Steck, 1992) contain several parameters which in general cannot be determined explicitly from suitable experiments. Instead these parameters have to be determined implicitly from different measurement data. The main problem of the estimation of these parameters derives from the *numerical stiffness* of the underlying constitutive equations (see, e.g. Cordts and Kollmann, 1986; Hartmann and Kollmann, 1987). Therefore the topic of the present paper is the estimation of the model parameters with a focus on the solution of the numerical problem.

Most material data are from uniaxial or biaxial experiments, which performed, for example, for cylindrical hollow specimens lead to (almost) uniform strains and stresses within the specimens (see, e.g. Krempl and Lu, 1984; White et al., 1990; Schinke and Schwertel, 1994; Kunkel and Kollmann, 1997). There are only a few authors who have published results for specimens with a non-homogeneous distribution of strain and stress (see Cailletaud and Pilvin, 1993; Gavrus et al., 1994; Andresen et al., 1996; Kreißig, 1996; Mahnken and Stein, 1994b, 1996b, 1997). Due to the high costs, the number of experiments is always limited. No statistical proofed results have been published yet. Also, the influence of deviation in the measurement data on the model parameters is still an open question (see, e.g. Schinke and Schwertel, 1994; Braasch et al., 1995; Gerdes and Thielecke, 1996). The main question is the reliability of the material models. Only in the case of a small standard deviation of the model parameters one can expect a more or less 'exact' prediction of the material behaviour under the prescribed loads. For this reason the determination of standard deviation and correlation of the model parameters will be discussed in detail.

Another important problem is the difficulty of getting adequate starting values or even the range of the model parameters. Although the principal influence of the parameters on the model behaviour is known in advance, it is almost impossible to give those values without a time-consuming stochastic search method. To shorten the CPU-time one can make use of a combination of stochastic and deterministic search algorithms. Very often the so-called evolution strategy is used to evaluate the material parameters (see, e.g. Rechenberg, 1973; Müller and Hartmann, 1989; Kublik and Steck, 1992; Furukawa and Yagawa, 1997). There is little experience with deterministic methods (see Senseny et al., 1993; Mahnken and Stein, 1994a, 1996a). Thus a great part of the present paper will deal with modern deterministic optimization methods and, particularly, how to provide the gradient of the cost function. In this respect the sensitivity analysis has become an effective method (e.g. Adelman and Haftka, 1986; Gavrus et al., 1994; Mahnken and Stein, 1994a, 1996a; Gelin and Ghouati, 1996).

The amount of CPU-time can also be reduced with simple parallel concepts. The search in a high-dimensional parameter space is implicitly parallel, allowing one to use a workstation cluster as a parallel virtual machine. There are also higher parallel concepts, which require a greater effort than the former one (see, e.g. Kreißig, 1996), which will also be discussed.

Determination of the parameters of any model constitutes an inverse problem (Bard, 1974; Banks and Kunisch, 1989; Bui, 1994), which often is related with instability problems (Morozov, 1984; Baumeister, 1987; Banks and Kunisch, 1989; Louis, 1989).

A number of authors have shown that time-integration of the constitutive equations with explicit algorithms also leads to numerical instabilities and have therefore used implicit methods (see, e.g. Cordts and Kollmann, 1986; Hartmann and Kollmann, 1987; Stein and Wriggers, 1989). However, explicit algorithms like the Runge–Kutta Dormand–Prince method are quite commonly used, because they do not require any Jacobian matrix, if no accompanying stability analysis is performed (see Mahnken and Stein, 1989). In this paper we present stable and accurate integration methods which avoid the above mentioned numerical problems. Only with these implicit methods the allowable time-steps are great enough to reduce the amount of CPU-time in large finite-element calculations (see Mahnken and Stein, 1989).

2. Modelling the inelastic material behaviour of metals

The need for an adequate description of the complex inelastic behaviour of modern metal alloys under monotonic and cyclic loading and high temperatures has created numerous constitutive models in the past two decades. Most of them are constructed in a way that they contain a purely elastic regime of hyper- and hypo-elastic behaviour, respectively. For the inelastic behaviour it is generally accepted that

$$\dot{\underline{\epsilon}}_i = f(\underline{\sigma}, T; q_m) \quad (1)$$

the inelastic part of the strain rates is a function of state variables stress $\underline{\sigma}$ and temperature T , and a set of internal variables q_m with evolutionary equations

$$\dot{q}_\ell = q_\ell(\underline{\sigma}, T; q_m), \quad (m, \ell = 1 \dots n) \quad (2)$$

representing the history of the inelastic process.

Although there exist a number of models for the description of the elastic–plastic and the elastic–viscoplastic response of metallic materials like austenitic steels [e.g. the models of Bodner and Partom, Chaboche, Hart, Krempl, Miller, Steck, etc. (see, e.g. Eftis et al., 1989; Chaboche and Rousselier, 1983; Krempl, 1987; Miller, 1987; Nouailhas, 1989; Kublik and Steck, 1992)], in this paper we have chosen the Interatom-model (IA-model) for analysis purposes. This model has been developed to describe the behaviour of the austenitic steels SS 304 and 316L (see Bruhns, 1984; Bruhns and Pitzer, 1987), and is introduced in the Appendix. Moreover, with Bruhns and Rott (1994) a general frame has been introduced for the description of the elastic–plastic and the elastic–viscoplastic response of austenitic steels.

The above mentioned models contain a certain number of parameters, and these parameters have to be determined from a limited number of experiments. However,

all models share the same problems with the estimation of these parameters, namely the numerical stiffness of the constitutive equations. The general results for the IA-model presented in this paper are therefore also applicable to the other models.

3. Numerical methods to determine the model parameters

The following section is divided in two subsections. The first one, called the *direct problem*, deals with the numerical simulation of the experiments. The second one, the *inverse problem*, shows how to solve the problem of estimating the model parameters (for an overview see, e.g. Tarantola, 1987; Bui, 1994; Bui et al., 1994).

3.1. Direct problem

In this paper we discuss the results for specimens with a uniform distribution of stresses and strains from uniaxial tests. In this case the direct problem is reduced to the time-integration of the uniaxial constitutive equations (A8), (A15) and (A24). These equations fit into the general form:

$$\dot{\vec{y}} = \vec{F}(\vec{y}(t)), \quad \vec{y} = \begin{pmatrix} \varepsilon \\ q_1 \\ \vdots \\ q_m \end{pmatrix}, \quad t_0 \leq t \leq t_e \quad (3)$$

with the initial values at time t_0

$$\vec{y}(t_0) = \vec{y}_0. \quad (4)$$

Eq. (3) describes a system of first order ordinary differential equations with a solution vector \vec{y} . This vector contains the strain ε and the internal variables q_1, \dots, q_m of the model. The task is to find this vector for any time $t \leq t_e$.

The two main requirements for this calculation are *stability* and *accuracy*. It will be shown that even very accurate integration methods like the Runge–Kutta Dormand–Prince method (see, e.g. Press et al., 1992; Rentrop et al., 1996) do not lead to satisfactory results because of numerical instabilities. One step methods as used in this paper are of order p , if with $\vec{y}_0 = \vec{y}_0$

$$\vec{y}_1 - \vec{y}(t_0 + \Delta t_0) = \mathcal{O}(\Delta t_0^{p+1}) \quad \text{for } \Delta t_0 \rightarrow 0 \quad (5)$$

holds for the local discretization error (error after one step) (see Lambert, 1983; Rentrop et al., 1996). The notation \mathcal{O} defines the magnitude of the discretization error. A high order p of the integration method will lead to low discretization errors.

A high accuracy, however, is not sufficient to solve the differential equations of the type (3), because the model is *stiff*, as demonstrated below. The stiffness of other

models for viscoplastic material behaviour has been shown by a number of authors (see, e.g. Cordts and Kollmann, 1986; Hartmann and Kollmann, 1987; Senseny et al., 1993). Therefore, the following statements hold for all these models.

The stability term for stiff differential equations is introduced for the scalar equation, Rentrop et al. (1996)

$$\dot{y} = \lambda y, \quad \text{Re} \lambda \leq 0. \tag{6}$$

There is also a general approach for systems of type (3), so that the following statements hold for both Eqs. (6) and (3). Single-step methods approximate the solution of Eq. (6) with

$$\tilde{y}_n = [R_0(z)]^n \tilde{y}_0, \quad z = \Delta t_n \lambda. \tag{7}$$

In Eq. (7) the term $R_0(z)$ defines the *stability function*. A single-step method is said to be *A-stable*, if $|R_0(z)| \leq 1 \forall \text{Re } z \leq 0$ holds, i.e. the approximate solution remains in fixed boundaries. The method is said to be *L-stable*, if it is A-stable and $\lim_{\text{Re } z \rightarrow -\infty} R_0(z) = 0$ holds, i.e. the approximate solution tends to zero for large z , as the true solution does.

The stability function of an *explicit method* is a polynomial in Δt_n . For this reason explicit methods only have a finite region of absolute stability, the so-called *stability region*, which is a strong restriction for the allowable stepsize Δt_n . *Implicit methods* like the Crank–Nicolson method used in this paper are A-stable and therefore do not have any restriction for the stepsize. This is a great advantage, because the allowable stepsize for an explicit method can lead to unsatisfactory small steps (see Mahnken and Stein, 1989).

To demonstrate the violation of the stability region, consider the following example: A monotonic tensile test with a constant strain rate of $\dot{\epsilon} = 10^{-2} \text{ s}^{-1}$ up to a total strain of 1% is simulated with the uniaxial form (A15) of the underlying model. Two integration methods are chosen; on the one hand the classical explicit fourth order Runge–Kutta method with an *adaptive stepsize*, on the other hand the above mentioned implicit second order Crank–Nicolson method. The adaptive stepsize control for the explicit method is performed in the following way. Starting with \tilde{y}_n two approximate values for $\tilde{y}(t_n + \Delta t_n)$ are determined; on the one hand the value \tilde{y}_{n+1} with the stepsize Δt_n , on the other hand the value \tilde{y}_{n+1} with two steps of the size $\frac{\Delta t_n}{2}$. The difference of the values is an error estimate (see Mahnken and Stein, 1989). For the explicit method the stepsize influences both stability and accuracy, for the implicit method only accuracy. To improve the accuracy of the Crank–Nicolson method we have implemented the fractional step algorithm of order 3, but not changed the stepsize. This saves CPU time compared to an adaptive stepsize control like that for the explicit method. It should be noted, that also implicit methods can lead to wrong results, if not a proper control of the stepsize w.r.t. accuracy is applied, but the following example shows that the Crank–Nicolson method works well without a stepsize control.

To test the stability of the two methods, the overstress-parameter $\gamma(T)$ from Eq. (A15) is changed within the range of 10^{-40} – 10^{-10} s^{-1} . The following two pictures show a comparison between the results of the Crank–Nicolson method and the fourth-order Runge–Kutta method with adaptive stepsize (Figs. 1 and 2).

For the Crank–Nicolson method we have used a fixed stepsize of $\Delta t = 10^{-3} \text{ s}$. This was also the biggest stepsize for the adaptive stepsize control of the explicit method. The Crank–Nicolson method needed 1000 timesteps and 3000 iterations in the implicit integration scheme to integrate one monotonic test. The CPU time for the Crank–Nicolson method to integrate one monotonic test was 18 CPU s (depending on the computer used, therefore this value gives only a magnitude).

It can be seen that it is not possible to integrate the model within the full range of the parameters using an explicit method with an acceptable stepsize. The Crank–Nicolson method with a fixed stepsize, which is 1000 times higher than the smallest stepsize of the Runge–Kutta method, is stable even in the region of $\gamma(T) = 10^{-10} \text{ s}^{-1}$, where the model becomes extremely stiff. This shows the necessity of using an implicit integration method to determine the parameters of the model; any optimization method will fail with the wrong integration method.

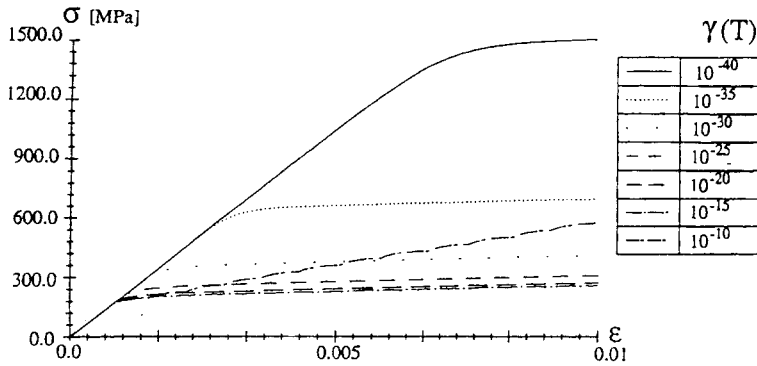


Fig. 1. Explicit time-integration with fourth-order Runge–Kutta method.

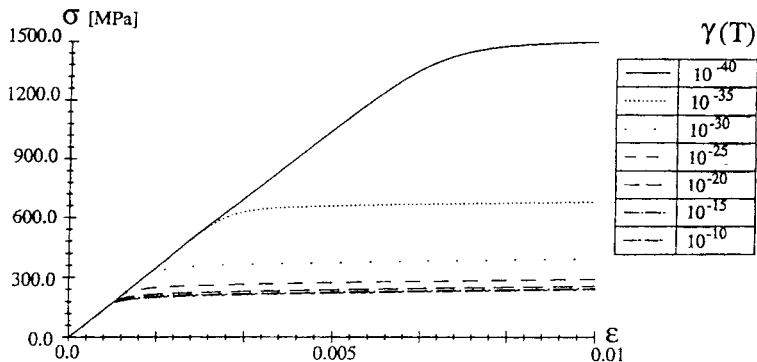


Fig. 2. Implicit time-integration with second-order Crank–Nicolson method.

This corresponds with the experiences of other authors in this field; e.g. Cordts and Kollmann (1986) showed the stiffness of the models of *Hart* and *Miller* and derived an implicit integration scheme for the governing equations. Stein and Wriggers (1989) pointed out that implicit integration methods are most commonly used nowadays.

3.2. Inverse problem

In the present paper the model parameters are estimated with the least-squares criterion. The basic assumption of this method is that the measurement errors follow a normal distribution. In this case, the certainty of a special set of parameters a_1, \dots, a_m of the model $y(x_i; a_1, \dots, a_m)$ being the right one is given as (Press et al., 1992)

$$\prod_{i=1}^n \left\{ e^{-\frac{1}{2}(y_i - y(x_i; a_1, \dots, a_m))/\sigma)^2} \Delta y \right\} \rightarrow \max \tag{8}$$

with the standard deviation σ at the points x_i . The maximization of the *likelihood-function* (8) is identical to the minimization of

$$\left[\sum_{i=1}^n \frac{(y_i - y(x_i; a_1, \dots, a_m))^2}{2\sigma^2} \right] - n \log \Delta y \rightarrow \min. \tag{9}$$

Introducing an individual standard deviation σ_i for all measured points x_i and a number l of nonlinear restrictions g_j on the model parameters $\vec{\mathbf{a}}$ the least-squares method is given as

$$f(\vec{\mathbf{a}}) = \frac{1}{2} \sum_{i=1}^n \frac{(y_i - y(x_i; a_1, \dots, a_m))^2}{\sigma_i^2} \rightarrow \min_{\vec{\mathbf{a}} \in G}, \tag{10}$$

with

$$G = \{ \vec{\mathbf{a}} \in \mathbb{R}^m : g_j(\vec{\mathbf{a}}) = 0, \quad j = 1, \dots, l_e, \quad g_j(\vec{\mathbf{a}}) \geq 0, \quad j = l_e + 1, \dots, l \}. \tag{11}$$

In vector notation the least-squares function has the short form

$$f(\vec{\mathbf{a}}) = \frac{1}{2} \vec{\mathbf{r}}(\vec{\mathbf{a}})^T \underline{\mathbf{G}} \vec{\mathbf{r}}(\vec{\mathbf{a}}), \quad \vec{\mathbf{r}} : \mathbb{R}^m \rightarrow \mathbb{R}^n, \quad n > m. \tag{12}$$

In the above equation $\vec{\mathbf{r}}(\vec{\mathbf{a}})$ defines the residual vector

$$\vec{\mathbf{r}}(\vec{\mathbf{a}})^T = (r_1(\vec{\mathbf{a}}), r_2(\vec{\mathbf{a}}), \dots, r_n(\vec{\mathbf{a}})), \quad r_i(\vec{\mathbf{a}}) = (y_i - y(x_i; a_1, \dots, a_m)), \tag{13}$$

$$i = 1, \dots, n$$

and the matrix $\underline{\mathbf{G}}$ contains the standard deviations σ_i

$$G_{ii} = \frac{1}{\sigma_i^2}, \quad i = 1, \dots, n. \tag{14}$$

In the present case of the parameter identification of inelastic material models there also exist general nonlinear constraints for the model parameters due to the material functions used. These restrictions result from thermodynamic considerations on the material models (see, e.g. Lehmann, 1989). Therefore, in this paper methods for constrained optimization problems are used.

With Eq. (10) the optimization problem is defined, it can be solved with several methods (for an overview see, e.g. Großmann and Terno, 1993). Considered here are methods which take into account the special structure of the least-squares function, e.g. *Gauss–Newton methods* (Dennis and Schnabel, 1983).

The quadratic approximation of the least-squares function $f(\vec{\mathbf{a}})$ at the actual iteration point $\vec{\mathbf{a}}^k$ leads to the iteration scheme (Dennis and Schnabel, 1983),

$$\vec{\mathbf{a}}^{k+1} = \vec{\mathbf{a}}^k - (\underline{\mathbf{J}}(\vec{\mathbf{a}}^k)^T \underline{\mathbf{J}}(\vec{\mathbf{a}}^k) + \underline{\mathbf{S}}(\vec{\mathbf{a}}^k))^{-1} \underline{\mathbf{J}}(\vec{\mathbf{a}}^k)^T \vec{\mathbf{r}}(\vec{\mathbf{a}}^k). \tag{15}$$

In Eq. (15) the matrix

$$J(\vec{\mathbf{a}})_{ij} = \frac{\partial r_i(\vec{\mathbf{a}})}{\partial a_j}; \quad \underline{\mathbf{J}}(\vec{\mathbf{a}}) \in IR^{n \times m} \tag{16}$$

defines the *Jacobian* and the matrix

$$\underline{\mathbf{S}}(\vec{\mathbf{a}}) = \sum_{i=1}^n r_i(\vec{\mathbf{a}}) \nabla^2 r_i(\vec{\mathbf{a}}) \tag{17}$$

contains the second derivatives of the least-squares function. With this *full Newton method* local quadratic convergence is achieved

$$\|\vec{\mathbf{a}}^{k+1} - \vec{\mathbf{a}}^*\| \leq c \|\vec{\mathbf{a}}^k - \vec{\mathbf{a}}^*\|^2 \quad \forall k \geq \hat{k} \geq 0, \quad c \geq 0. \tag{18}$$

Because of the difficulty to derive the second order derivatives of the least-squares function the *Gauss–Newton method* is used. The local quadratic convergence Eq. (18) only holds if the second order derivative is demonstrated to be negligible, i.e. $\underline{\mathbf{S}}(\vec{\mathbf{a}}) \approx \mathbf{0}$ holds throughout the iteration.

A special form of the Gauss–Newton method is introduced to include restrictions on the model parameters and to bring in damping in a natural way. This method solves a *quadratic program* in every iteration step with the method of Wolfe (Collatz and Wetterling, 1966).

Another way to solve the optimization problem (10) is shown by Schittkowski (1981). The basic idea of the method is the transformation of the restricted problem into an unconstrained optimization problem. The solution of a quadratic sub-problem

$$\frac{1}{2} \vec{\mathbf{d}}^T \nabla_{xx}^2 L(\vec{\mathbf{a}}^k, \vec{\mathbf{u}}^k) \vec{\mathbf{d}} + \nabla f(\vec{\mathbf{a}}^k)^T \vec{\mathbf{d}} \rightarrow \min_{\vec{\mathbf{d}} \in G} \tag{19}$$

with linear restrictions

$$\begin{aligned} G = \{ \vec{\mathbf{d}} \in \mathbb{R}^m : g_j(\vec{\mathbf{a}}^k) + \nabla g_j(\vec{\mathbf{a}}^k)^T \vec{\mathbf{d}} = 0, \quad j = 1, \dots, l_e, \\ g_j(\vec{\mathbf{a}}^k) + \nabla g_j(\vec{\mathbf{a}}^k)^T \vec{\mathbf{d}} \geq 0, \quad j = l_e + 1, \dots, l \} \end{aligned} \tag{20}$$

defines the search direction in the parameter space. In Eq. (19)

$$L(\vec{\mathbf{a}}, \vec{\mathbf{u}}) := f(\vec{\mathbf{a}}) - \sum_{j=1}^l u_j g_j(\vec{\mathbf{a}}) \tag{21}$$

defines the Lagrange function. Schittkowski (1981) uses the iteration scheme

$$\begin{pmatrix} \vec{\mathbf{a}}^{k+1} \\ \vec{\mathbf{v}}^{k+1} \end{pmatrix} = \begin{pmatrix} \vec{\mathbf{a}}^k \\ \vec{\mathbf{v}}^k \end{pmatrix} + \alpha_k \begin{pmatrix} \vec{\mathbf{d}}^k \\ \vec{\mathbf{u}}^k - \vec{\mathbf{v}}^k \end{pmatrix}, \quad k = 0, 1, \dots \tag{22}$$

Herein $(\vec{\mathbf{a}}^k, \vec{\mathbf{v}}^k)^T$ defines the solution vector of the *merit function*:

$$\begin{aligned} \Phi(\vec{\mathbf{a}}, \vec{\mathbf{v}}) = f(\vec{\mathbf{a}}) + \sum_{j=1}^{l_e} v_j g_j(\vec{\mathbf{a}}) + \frac{1}{2} r g_j(\vec{\mathbf{a}})^2 \\ + \sum_{j=l_e+1}^l \begin{cases} v_j g_j(\vec{\mathbf{a}}) + \frac{1}{2} r g_j(\vec{\mathbf{a}})^2, & g_j(\vec{\mathbf{a}}) \geq -\frac{v_j}{r} \\ -\frac{1}{2} \frac{v_j^2}{r}, & \text{else} \end{cases} \end{aligned} \tag{23}$$

The main characteristic of merit functions is the congruence of the minimum of the cost function $f(\vec{\mathbf{a}}^*)$ and the first component of the saddle point $(\vec{\mathbf{a}}^*, \vec{\mathbf{v}}^*)^T$. With Eq. (23) an unconstrained optimization problem is defined.

All the methods mentioned above require information about the slope of the cost function and the first derivative of the functions g_j . Therefore an important task is the calculation of the first order derivatives of the least-squares sum $f(\vec{\mathbf{a}})$. As no analytical solution of the least-squares problem (10) exists, the gradient can only be approximated, e.g. via secant approximation. The other way is to derive the gradient of the least-squares function analytically with respect to the underlying time integration

scheme (see, e.g. Mahnken and Stein, 1996a). This way, however, is not considered here. All approximation methods lead to the well known *stepsize dilemma*, which results from the contrariety of *discretization errors* and the *truncation or rounding errors* (see, e.g. Braess, 1997).

A way to overcome this dilemma is shown in Anding (1997); a proper individual stepsize h_j for each parameter a_j can be calculated with the simple formula

$$h_j = \sqrt{\eta} \max(|a_j|, \text{typ}(a_j)) \text{sign}(a_j). \tag{24}$$

In Eq. (24)

$$\text{typ}(a) = \begin{cases} 10^{\text{int}(\log_{10}(|a|)+0.30103)}, & \text{if } |a| \geq 1 \\ 10^{\text{int}(\log_{10}(|a|)-0.69897)}, & \text{if } 0 < |a| < 1 \end{cases} \tag{25}$$

defines the magnitude of the parameter a and η the error bound for truncation and rounding errors. As the function value $f(\vec{a})$ results from the solution of a system of first order differential equations, the error bound η depends strongly on the accuracy of the integration method used. Therefore no global estimate can be given. In the present paper a stepsize $h_j = 10^{-2} \max(|a_j|, \text{typ}(a_j)) \text{sign}(a_j)$ was found to be best.

The above mentioned optimization methods converge very fast when near a minimum of the cost function. Normally one has little knowledge of the function, so that the initial values for the model parameters are often far away from the optimum. In this case, stochastic search methods help to find parameter values near the optimum. A great advantage of these methods are the low requirements on the cost function; it needs neither to be continuous nor differentiable. Therefore no gradient evaluation is necessary. The greatest disadvantage is the amount of CPU-time.

Modern stochastic search methods are divided in two groups; the first one contains *genetic algorithms*, which deal with binary numbers, the second one is called *evolution strategies*, these methods are using real numbers for optimization. For an overview about these methods see Schöneburg et al. (1994). A comparison between evolution strategies and genetic algorithms is shown in Schwefel et al. (1994); the result is that for continuous cost functions evolution strategies are best. In the case of discontinuous functions genetic algorithms have the better performance. Based on these results we have chosen evolution strategies.

The success of the evolution search depends strongly on the handling of the step-size during the optimization. A highly sophisticated way to solve this problem is shown in Ostermeier et al. (1994):

$$\vec{a}_C^g = \vec{a}_P^g + \delta^g \delta_{\text{scal}}^g \vec{z}$$

$$\vec{z}^g = \left(1 - \frac{1}{\sqrt{m}}\right) \vec{z}^{g-1} + \frac{1}{\sqrt{m}} \vec{z}$$

$$\delta^{g+1} = \delta^g \left(\exp \left(|\bar{\mathbf{z}}^g| \left(\frac{\sqrt{m}}{2\sqrt{m}-1} \right)^{-\frac{1}{2}} - 1 + \frac{1}{5m} \right) \right)^{\frac{1}{m}}$$

$$\bar{\delta}_{\text{scal}}^{g+1} = \bar{\delta}_{\text{scal}}^g \left(|\bar{\mathbf{z}}^g| \left(\frac{1}{2\sqrt{m}-1} \right)^{-\frac{1}{2}} + 0.35 \right)^{\frac{1}{m}}.$$
(26)

Herein the index C defines the children, the index P the parents and the index g the actual generation. Small variations of the parameters are introduced via normal distributed random numbers $\bar{\mathbf{z}}$ with the mean value 0 and the standard deviation $\sigma = 1/\sqrt{m}$ (m = number of parameters). These random numbers are multiplied with a global stepsize δ^g and an individual stepsize $\bar{\delta}_{\text{scal}}^g$ for each parameter. The stepsize parameters are changed with regard to information from previous optimization steps. To handle the nonlinear restrictions (11) in the evolution strategy penalty methods are used (see, e.g. Großmann and Terno, 1993). Due to an increasing penalty parameter non feasible parameters do not survive in the evolution.

To overcome the problem of large CPU-times, one can make use of the implicit parallelism of the evolution strategy (see Schöneburg et al., 1994). A popular concept in this context is the so called *Master–Slave paradigm*:

A pool of tasks is defined, in this case, the total number of evolutions (see, e.g. Geist et al., 1994). The master checks the termination criterion, if there are any tasks left or if the value of the cost function is already small enough to stop the search. Furthermore, the master distributes the best parameter set over the network and therefore has the control over all evolutions. The slaves do the work; this means the evaluation of the cost function and the variation of the parameters. The number of evolution runs is also distributed by the master. There is some experience with the Master–Slave concept in the context of the simultaneous estimation of model parameters used in constitutive equations. In this paper the program PVM is used to organize the concept in a heterogeneous network.

Another important aspect of the estimation of the parameters of constitutive equations is the reliability of the model parameters. Only in case of small standard deviations of the parameters the predictions made with the model can be accurate, otherwise the results are too vague to rely upon. This demonstrates that the estimation of the model parameters is not enough, also the sensitivity of the parameters has to be calculated (Press et al. 1992).

The sensitivity of the model parameters is specified with the *covariance matrix* $\underline{\mathbf{C}}$ of the least-squares sum

$$f(\bar{\mathbf{a}}) = \frac{1}{2} \bar{\mathbf{r}}(\bar{\mathbf{a}})^T \underline{\mathbf{G}} \bar{\mathbf{r}}(\bar{\mathbf{a}})$$

$$\underline{\mathbf{C}} = \nabla^2 f(\bar{\mathbf{a}})^{-1}.$$
(27)

The covariance matrix can be calculated with the first order derivatives of the model y at each point x_i (Press et al., 1992)

$$\frac{\partial^2 f(\vec{\mathbf{a}})}{\partial a_k \partial a_l} \approx \sum_{i=1}^n \frac{1}{\sigma_i^2} \left(\frac{\partial y(x_i; a_1, \dots, a_m)}{\partial a_k} \frac{\partial y(x_i; a_1, \dots, a_m)}{\partial a_l} \right). \tag{28}$$

To specify the correlation between the model parameters the *correlation coefficient*

$$\rho(a_i, a_j) = \frac{C_{ij}}{\sqrt{C_{ii}C_{jj}}}; \quad -1 \leq \rho(a_i, a_j) \leq +1 \tag{29}$$

is defined. In case of $|\rho| = 1$ the parameters a_i and a_j are linear dependent, which means that there is no unique solution of the optimization problem. This also means that there is not enough information in the cost function. To overcome this situation, more measurement data is required. It should be stated here, that it is not only the quantitative amount of data which is important, but the quality of data. Therefore it becomes necessary to run a number of different tests to activate the different mechanisms intended by the model.

The calculation of the first order derivatives of the model is very difficult, as mentioned before. Therefore another popular way to get information about the sensitivity of the model parameters is the creation of *simulated data sets*. This requires the best knowledge about the uncertainty in the measurement data. Only in case of the right distribution the simulated data sets are a true surrogate for the original data. To demonstrate if the chosen distribution is correct or not, one can use the χ^2 -test (see Heinhold and Gaede, 1972). The way to create simulated data sets can be taken from Fig. 3.

The basis for the Monte Carlo simulation is the model with the best fitted parameters. Instead of the actual data set the model with the parameters $\vec{\mathbf{a}}_0$ is chosen. At each measurement point x_i a synthetic data point is created with the right distribution, e.g. a white noise. The minimization of the least-squares sum delivers

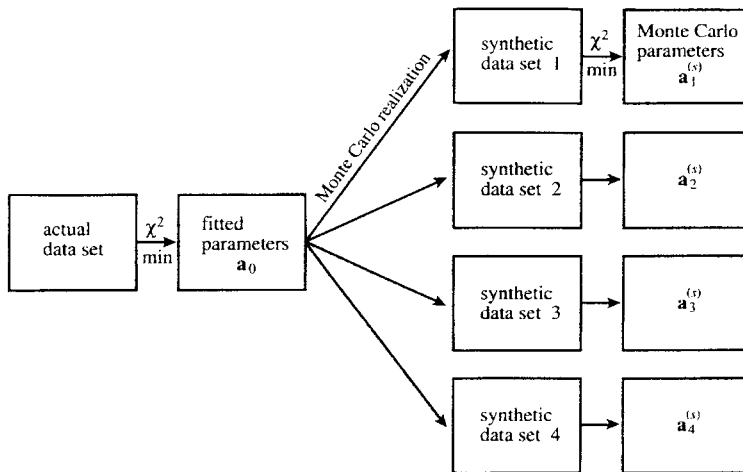


Fig. 3. Monte Carlo simulation of an experiment (source: Press et al., 1992).

Monte Carlo parameters $\tilde{\mathbf{a}}_i^{(s)}$. The distribution of these parameters gives then the information about the sensitivity of the model parameters. In the case of normal distributed measurement errors there is a clear defined conjunction between the standard deviation and the *confidence regions* on the parameters.

4. Numerical results for stainless steel SS 304

The parameters of the model, Eqs. (A8), (A15) and (A24), are all estimated from uniaxial tests. The test data are taken from Westerhoff (1995). The strategy to find these parameters was proposed by Bruhns and Pitzer (1987). These authors classify the temperature dependent parameters of the model in three categories:

- i. parameters for the elastic response of the material, e.g. Young’s modulus E ,
- ii. parameters of the rate independent theory, e.g. the initial yield stress σ_F and the tangent modulus E_t and
- iii. parameters to describe the viscous effects.

The parameters presented in this paper are for a SS 304 (1.4948 according to German standards) at room temperature. The model is also capable of reproducing the material behaviour at elevated temperatures, up to 600°C. The parameters for the higher temperature level are printed in Anding (1997). The evaluation of the parameters of the first category is also shown in detail in Anding (1997). Starting here with the parameters of the second category, one first has to estimate the parameters of Eq. (A12) to describe the hardening behaviour of SS 304 in monotonic tensile tests. This behaviour was, for example, measured by Westerhoff (1995) in six tests with a quasistatic strain rate (see Fig. 4).

In this case it is possible to give a value for the variance of the measured stress at fixed reference points ε (see Fig. 5). But for only six tests the basis for a statistic analysis is very small. This leads to another way to estimate the variance of the measured stresses; if the least-squares fit is best and all measured points have the

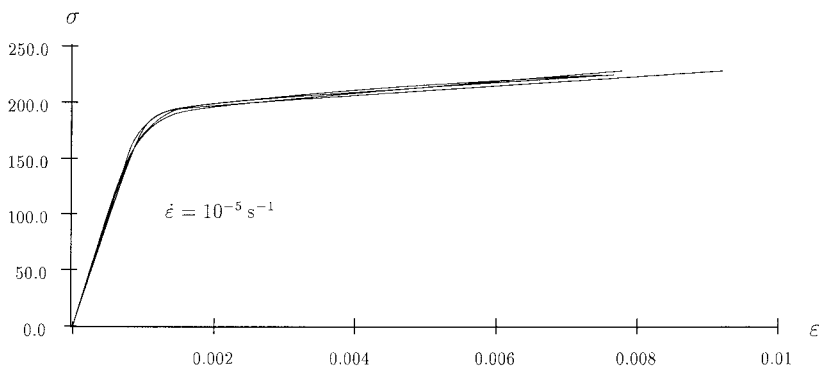


Fig. 4. Monotonic tensile tests with a quasistatic process velocity (source: Westerhoff, 1995).

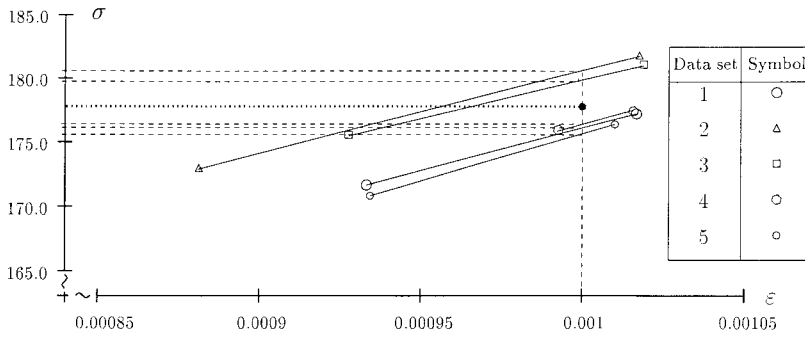


Fig. 5. Variance of the measured stress at a reference point $\epsilon = 0.1\%$ and mean value ●.

same distribution the variance can be estimated with the a posteriori value (see Press et al., 1992)

$$S^2 = \sum_{i=1}^n \frac{(y_i - y(x_i; a_1, \dots, a_m))^2}{n - m}. \tag{30}$$

The method to estimate the quasistatic parameters is here the Gauss–Newton method. Because all parameters are measurable quantities it is easy to give good starting values for the least-squares fit. The result of the optimization is shown in Fig. 6.

In Fig. 7 it can be seen that the residuals are normal distributed after the best least-squares fit. The frequency $m(i)$ of a special value of the residual is very close to the frequency $n * p(i)$ of the normal distribution. The χ^2 -test shows a value of 6.401 for a largest possible value $\chi^2_{\alpha=0.05} = 7.815$ so that one can use the normal distribution.

This leads to the variance of the stresses: $S_\sigma = 0.68$ MPa. With this variance we have created a white noise. In Table 1 the results of 1000 Monte Carlo simulations are shown.

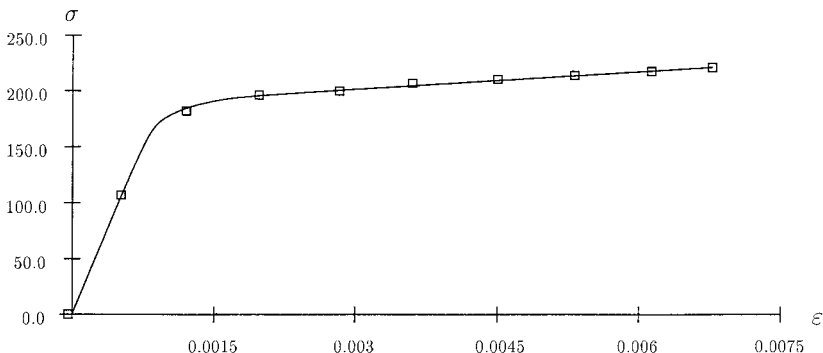


Fig. 6. Best fit of the IA-model.

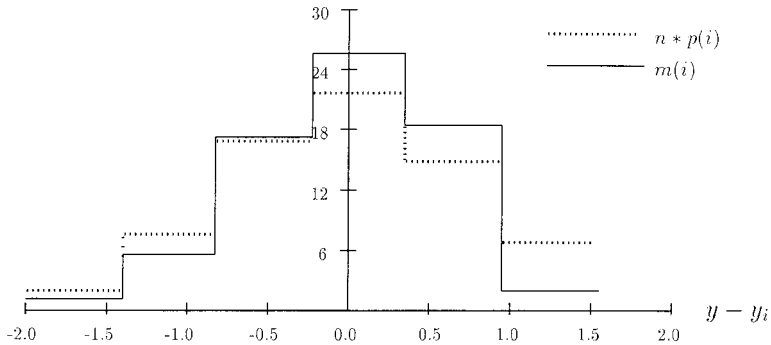


Fig. 7. Distribution of the residuals for the best fit.

Table 1
Mean value and variance of parameters E_{t0} , $E_{t\infty}$ and c_3 of the rate independant model

Data set	E_{t0} (MPa)	$E_{t\infty}$ (MPa)	c_3 (MPa)
1	193 785 ± 2904	4013 ± 33	196.1 ± 0.2
2	138 032 ± 2286	2973 ± 28	200.1 ± 0.2
3	183 256 ± 5094	3244 ± 36	198.7 ± 0.1
4	144 750 ± 2104	3045 ± 112	198.4 ± 0.5
5	170 590 ± 2305	3411 ± 5	198.9 ± 0.1
6	167 885 ± 1292	3187 ± 6	198.9 ± 0.1
$\bar{x} \pm S_x$	166 383 ± 21 575	3312 ± 376	198.5 ± 1.3

The variance of the parameter E_{t0} is rather high. On the other hand, the variance of c_3 is quite low, so that the parameters are suitable to predict the hardening of the material in monotonic tensile tests.

The next task is to determine the parameters for cyclic plasticity. The model has two hardening functions (A9) and (A10) to describe this behaviour. The measurement data are shown in Fig. 8. There are three cyclic tests with a constant strain rate of $\dot{\epsilon} = 10^{-5} \text{ s}^{-1}$. The maximum strain varies from 0.25 to 1.0%.

In this special case of only two model parameters c_1 and c_2 it is possible to evaluate the shape of the least-squares sum (see Fig. 9). It can be seen that the two parameters are highly correlated. The least-squares sum is not a convex function. The minimum of the cost function lies in a long valley with only a little slope on the ground. This shows the necessity to modify the hardening functions (A9) and (A10) of the model, because the underlying measurement data in Fig. 8 should be sufficient to identify the parameters for the hardening behaviour of the model. The optimization of the hardening functions is not part of the present paper, thus we will stay with the functions (A9) and (A10). For these two special functions thermodynamic considerations lead to the nonlinear restriction for the parameters c_1 and c_2 (see Anding, 1997):

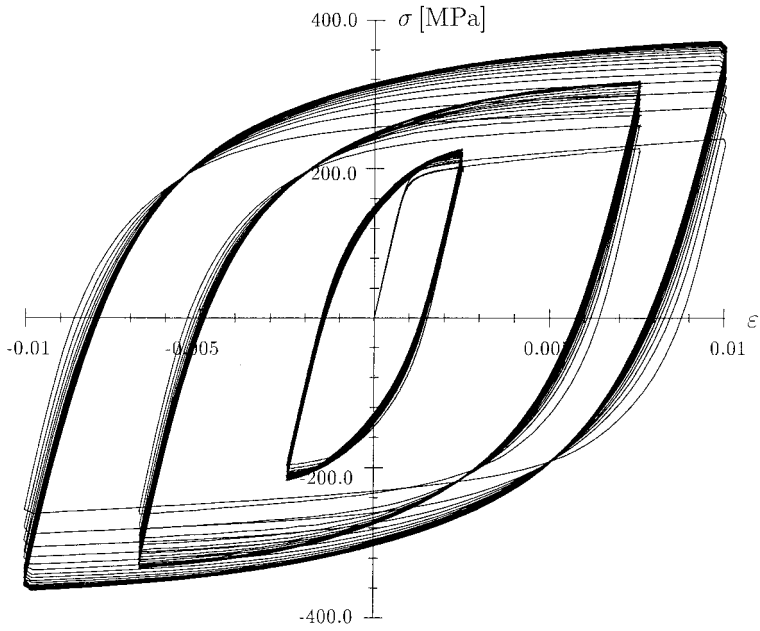


Fig. 8. Cyclic tests with a quasistatic strain rate of $\dot{\epsilon} = 10^{-5}$ (source: Westerhoff, 1995).

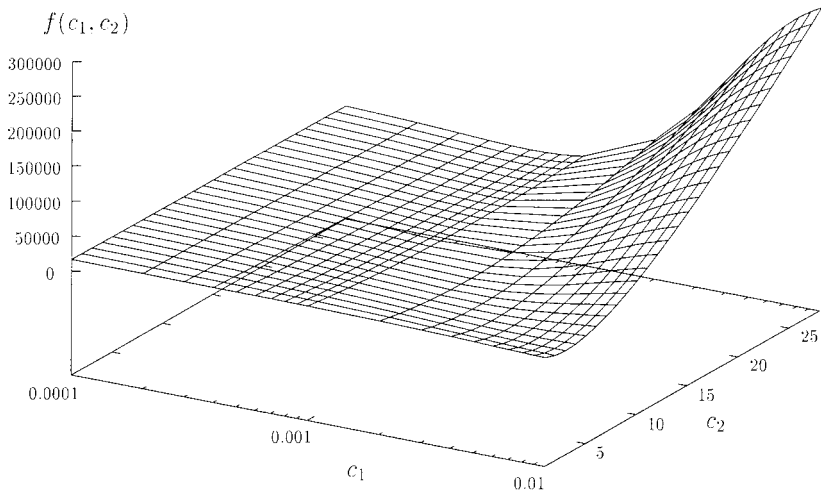


Fig. 9. Least-squares sum obtained from cyclic tests.

$$0 < c_1 < \frac{1}{(c_2 - 1) \cdot \sigma_F^2} \cdot \left[\frac{2 \cdot E_{t0}}{1 - \frac{E_{t0}}{E}} - 2 \cdot E_{t\infty} \right], \quad c_2 > 1. \tag{31}$$

The explanation for the parameters σ_F , E , E_{t0} and $E_{t\infty}$ is given in the Appendix A in Fig. A1.

To get good starting values for the optimization we have chosen the evolution strategy. To reduce the amount of CPU time we have implemented the Master–Slave concept and used 12 workstations for the search. This means that 12 cycles can be simulated with the model at the same time and therefore 12 sets of parameters can be checked at the same time. To get an impression of the resulting *speed up* see, e.g. Anding (1997). Due to the heterogeneous network we have also implemented a dynamic load balancing to avoid workstations running idle.

The success of the evolutionary search can be seen in Fig. 10. The evolution strategy follows exact the slope of the valley in Fig. 9. With this initial values it is easy to find the minimum of the least-squares sum. Because of its good performance we have chosen the method of Schittkowski (1981). The result of this optimization is shown in Fig. 11.

The model is capable of reproducing the cyclic behaviour of SS 304. The estimated parameters at room temperature are:

$$c_1 = 0.01991 \text{ MPa}^{-1}, \quad c_2 = 3.06412.$$

The standard-deviations of the parameters are small:

$$\sigma(c_1) = 2.5\%, \quad \sigma(c_2) = 0.5\%.$$

Due to the shape of the least-squares-sum the two parameters are highly correlated (see Table 2).

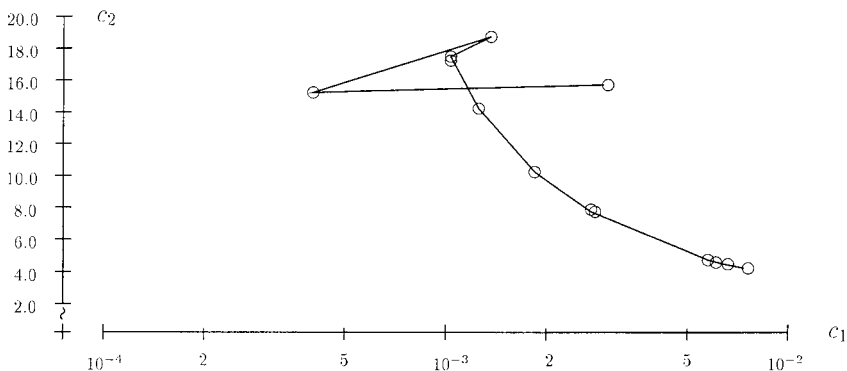


Fig. 10. Finding initial values for the parameters with the evolution strategy.

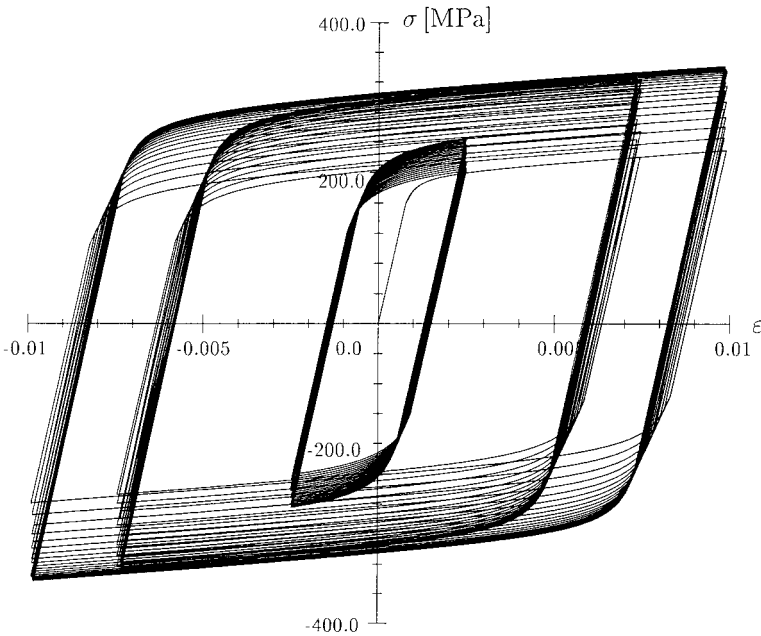


Fig. 11. Fit of the IA-model to cyclic tests.

Table 2

Correlation coefficients of parameters c_1 and c_2

ρ	c_1	c_2
c_1	1.0	-0.81
c_2	-0.81	1.0

The last task is the evaluation of the rate dependent parameters of the model in Eqs. (A15) and (A24). Therefore monotonic tensile tests with various strain rates, creep and relaxation tests are used (see Figs. 12–14).

For the three parameters γ , c_4 , c_5 of the overstress function in Eq. (A15) it is hard to give initial values. This makes it again necessary to use the evolution strategy. As before, we have used parallelization to reduce the amount of CPU time. To check the efficiency of the strategy we have made a comparison between the ‘+’-strategy and the ‘;’-strategy. In case of the ‘+’-strategy the parents remain in the optimization process, for the ‘;’-strategy they are deleted. For further details of this problem, see, Schöneburg et al. (1994). The result of this comparison is shown in Fig. 15.

It can be seen that the ‘;’-strategy converges much faster. Therefore we have always chosen this method.

To improve the parameters the method of Schittkowski (1981) was applied. The following values for the three parameters at room temperature were obtained:

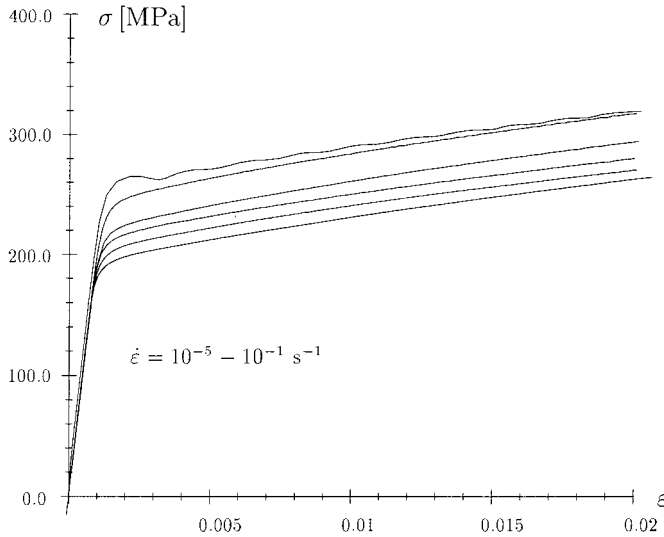


Fig. 12. Monotonic tensile tests with various strain rates (source: Westerhoff, 1995).

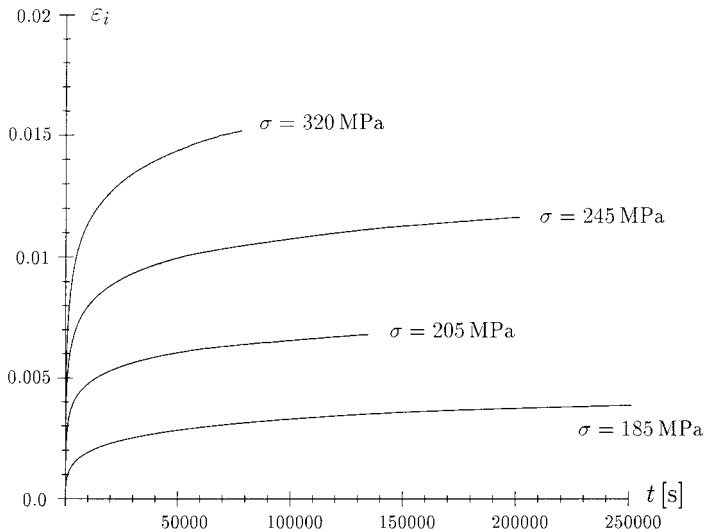


Fig. 13. Creep tests at various stress levels (source: Westerhoff, 1995).

$$\gamma = 6.9 \times 10^{-22} \text{ s}^{-1}, \quad c_4 = 1.0 \times 10^{-4} \text{ MPa}, \quad c_5 = 3.763.$$

Although the reproduction of the monotonic tests and the creep tests is good, the standard-deviations of the parameters are rather high:

$$\sigma(\gamma) = 189.1\%, \quad \sigma(c_4) = 52.65\%, \quad \sigma(c_5) = 0.5\%.$$

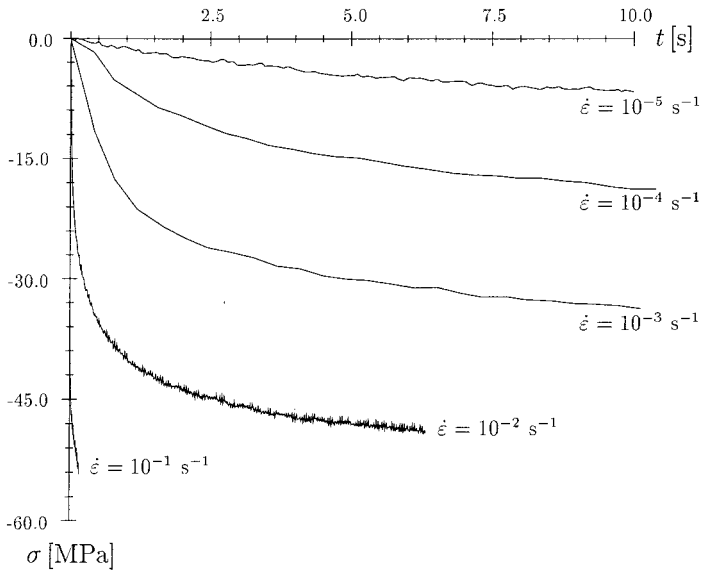


Fig. 14. Relaxation tests with various strain rates (source: Westerhoff, 1995).

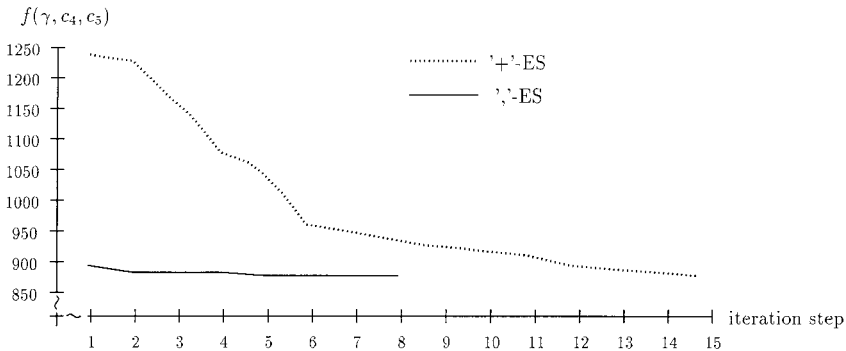


Fig. 15. Comparison between the '+'-evolution strategy and the ','-strategy.

The correlation-coefficients are shown in Table 3. It can be seen that it is necessary to bring in additional information into the optimization problem, e.g. via combined tension–torsion tests. With these multiaxial tests it should be possible to reduce the linear dependency of the parameters.

This shows, that, even with the best optimization tools, it is not possible to correctly obtain parameters — here γ and c_4 — which role is to model a phenomenon — here rate dependent material behaviour — insufficiently sensibilized in the considered experimental data. A further discussion on that point is made in Anding (1997).

For a better modelling of the rate dependent behaviour of the present austenitic steel the IA-model in the form (A24) is fitted to the tests of Figs. 12–14. The model

Table 3
Correlation coefficients of parameters γ , c_4 and c_5

ρ	γ	c_4	c_5
γ	1.0	0.99	-0.23
c_4	0.99	1.0	-0.12
c_5	-0.23	-0.12	1.0

contains 22 parameters for the viscoplastic behaviour, which all have to be determined simultaneously. In this paper, this was the biggest number of parameters to be optimized in one single optimization job. As before, the start parameters were determined with the parallelized evolution strategy. These start parameters were optimized with the method of Schittkowski. The least-squares function contained all the test data from Figs. 12–14, therefore one function evaluation was to integrate all monotonic tensile tests, all creep tests and all relaxation tests. The method of Schittkowski (1981) needed 40 iterations. During these iterations there were 84 function evaluations for the line search and 40 calculations of the gradient of the least-squares function, this means 880 function evaluations. Altogether these are 964

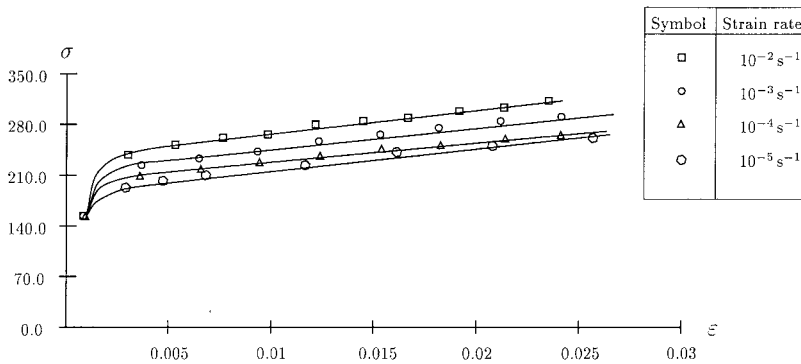


Fig. 16. Fit of the extended IA-model to monotonic tensile tests with various strain rates.

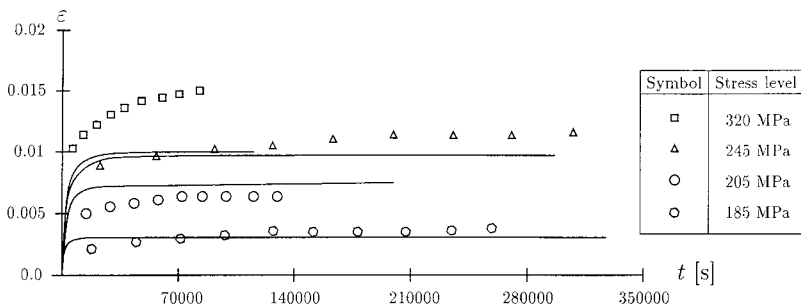


Fig. 17. Fit of the extended IA-model to creep tests at various stress levels.

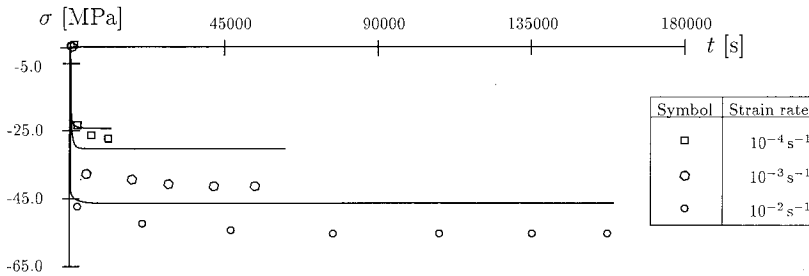


Fig. 18. Fit of the extended IA-model to relaxation tests with various strain rates.

integrations of all the tests in Figs. 12–14. These values give an impression of the effort required to optimize material parameters. The results of this least-squares fit is shown in the following pictures. A complete list of the parameters in Eq. (A24) is given in the Appendix A.

From Fig. 16 it can be seen that the extended IA-model gives an excellent reproduction of the monotonic tests, whereas the prediction of the creep and relaxation behaviour in Figs. 17 and 18 requires further improvement on the model. This indicates that the mechanisms of this kind of material behaviour are not fully included in the IA-model. Further extensions of the model seem to be necessary. But even in the form (A24) the IA-model should give good results for the prediction of complex structures under mechanical loads.

5. Conclusion

A general approach for parameter identification in the context of constitutive laws for modelling inelastic material behaviour is presented. The underlying experiments are uniaxial. This strategy to determine the material parameters requires less effort than non-homogeneous experiments, for which the parameter identification is performed by means of the Finite-Element-Method.

For the solution of the direct problem stable and accurate integration methods are presented. Therefore no preliminary studies on the parameters are necessary. Almost any starting values are feasible. Restrictions on the parameters result only from thermodynamic considerations or the range of value of the material functions and are not introduced to avoid numerical problems. With the combination of stochastic and deterministic optimization methods it is possible to reach the desired optimum of the cost function within a short time. This CPU time is significantly reduced via parallelization of the stochastic methods.

A certain disadvantage of the uniaxial strategy, namely the lack of information in the experimental data, is shown by error estimates and confidence regions. With an increasing number of different experiments the uncertainties in the material parameters decrease significantly.

We believe that the general approach presented here is an effective tool to determine the parameters of constitutive laws for inelastic material behaviour.

Acknowledgements

This work was supported by grants of the German National Science Foundation (DFG) within the graduate program ‘Computational Structural Dynamics’. The support from the DFG is gratefully acknowledged.

Appendix: The INTERATOM-model

The model is based on the assumption that the material behaviour up to a certain limit is purely elastic, and only beyond this limit shows rate-dependent effects. For the description of this inelastic behaviour the concept of overstresses, first proposed by Perzyna (1977), has been introduced, e.g. in Bruhns (1984), Bruhns and Pitzer (1987) and Bruhns and Rott (1994), together with an underlying rate-independent theory of elastic–plastic processes. The basic idea of the model is to split the rate of deformation tensor into a reversible (elastic) and an irreversible part, which contains both rate-dependent and rate-independent effects

$$\underline{\dot{\epsilon}} = \underline{\dot{\epsilon}}_r + \underline{\dot{\epsilon}}_i \tag{A1}$$

Starting with the basic static theory, the assumption of incompressibility in the plastic range and a generalized von Mises yield condition give the following constitutive equations

$$\underline{\dot{\epsilon}}_r = \frac{1}{2G} \left(\underline{\dot{\sigma}} - \frac{\nu}{1 + \nu} \text{tr}(\underline{\dot{\sigma}}) \mathbf{I} \right) + \alpha \Delta \dot{T} \mathbf{I}, \tag{A2}$$

$$\underline{\dot{\epsilon}}_i = \frac{LC}{4fh} \left\langle \frac{\partial F}{\partial \underline{\sigma}} \right\rangle. \tag{A3}$$

Herein

$$F = f - g = (\underline{\sigma}' - \underline{\xi}) : (\underline{\sigma}' - \underline{\xi}) - g(\kappa, T) = 0 \tag{A4}$$

is the yield condition and

$$LC = \frac{\partial F}{\partial \underline{\sigma}} : \underline{\dot{\sigma}} > 0 \tag{A5}$$

defines the loading condition. Accordingly, the inelastic deformation can only occur if both yield condition and loading condition are fulfilled. This condition is indicated with the McCauley brackets

$$\langle X \rangle = \begin{cases} X, & \text{if } F = 0 \text{ and } LC > 0 \\ 0, & \text{else} \end{cases}. \tag{A6}$$

The quantity *h* in Eq. (A3) defines the hardening function. The loading history of the material is included in the model by two internal variables; the first $\underline{\xi}$ representing

kinematic hardening effects, the second κ describing the isotropic hardening of the material. The evolution equations for these variables are

$$\dot{\underline{\xi}} = c(\kappa, T)\dot{\underline{\varepsilon}}_i, \quad \dot{\kappa} = (\underline{\sigma}' - \underline{\xi}) : \dot{\underline{\varepsilon}}_i, \tag{A7}$$

respectively.

In the present paper, all material functions were determined from uniaxial static tests. Therefore the governing equations will be specialized to this case. This leads to the simple form

$$\begin{aligned} \dot{\sigma} &= E_t(\kappa)\dot{\varepsilon}, \\ \dot{\xi} &= c(\kappa)\left(1 - \frac{E_t(\kappa)}{E}\right)\dot{\varepsilon}, \\ \dot{\kappa} &= \sqrt{\frac{3}{2}}g(\kappa)\left(1 - \frac{E_t(\kappa)}{E}\right)|\dot{\varepsilon}| \end{aligned} \tag{A8}$$

with the tangent modulus $E_t(\kappa)$ and the two hardening functions $c(\kappa)$ and $g(\kappa)$. In Bruhns (1984) the following functions are given

$$g(\kappa, T) = \frac{2}{3}\sigma_F(T)^2(1 + (c_2(T) - 1)(1 - e^{-c_1(T)\kappa})) \tag{A9}$$

and

$$c(\kappa, T) = \frac{\frac{2}{3}E_t(\kappa, T)}{1 - \frac{E_t(\kappa, T)}{E(T)}} - \frac{1}{3}\sigma_F(T)^2(c_2(T) - 1)c_1(T)e^{-c_1(T)\kappa}. \tag{A10}$$

These functions have two degrees of freedom, namely the temperature-dependent material parameters $c_1(T)$ and $c_2(T)$. The tangent modulus $E_t[\kappa(\varepsilon), T]$ is introduced as a function of measurable quantities, as shown in Fig. A1, wherein $E = 205.73$ GPa (Young’s modulus) and $\nu = 0.278$ (Poisson’s ratio) are the parameters of the elastic behaviour of the material.

In Fig. A1, $\sigma_F = 159$ MPa defines the initial yield stress and E_{t0} the initial slope in the inelastic region. The two quantities c_3 and $E_{t\infty}$ determine the asymptotic linear hardening behaviour of the material. With the abbreviations

$$\begin{aligned} a &= E_{t\infty} \\ b &= c_3 \\ c &= \frac{\sigma_F}{E_{t0}}\left(c_3 - \sigma_F\left(1 - 2\frac{E_{t\infty}}{E}\right)\right) - \frac{\sigma_F}{E}\left(c_3 + \sigma_F\frac{E_{t\infty}}{E}\right) \\ d &= \frac{1}{E_{t0}}\left(c_3 - \sigma_F\left(1 - 2\frac{E_{t\infty}}{E}\right)\right) - \frac{\sigma_F}{E} \end{aligned} \tag{A11}$$

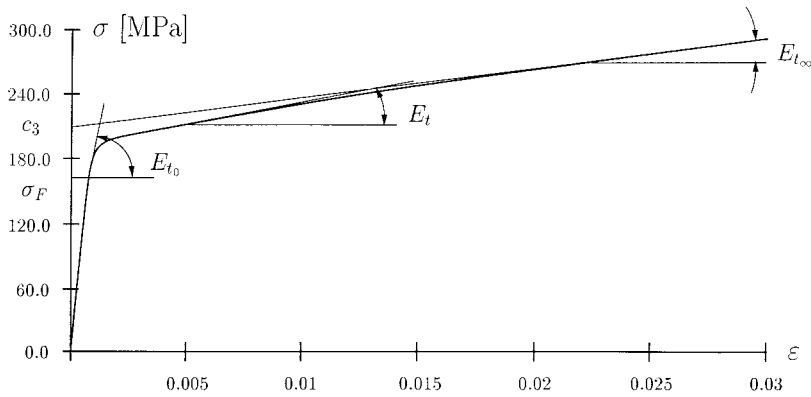


Fig. A1. Development of the tangent modulus $E_t(\kappa)$ during uniaxial tests.

the tangent modulus is given as

$$E_t = E_t[\kappa(\varepsilon), T] = \frac{d\sigma(\varepsilon)}{d\varepsilon} = a + \frac{d(b - ad) - c}{(d + \varepsilon)^2}. \tag{A12}$$

For a description of rate-dependent effects like creep and relaxation the concept of overstresses is used. With the actual stress $\underline{\sigma}$ and the associated stress $\underline{\sigma}$ on the yield surface the following expression is given for the inelastic strain-rate

$$\dot{\underline{\varepsilon}}_i = \ll \Phi(\Lambda, T) \gg \frac{\underline{\sigma}' - \underline{\xi}}{\sqrt{(\underline{\sigma}' - \underline{\xi}) : (\underline{\sigma}' - \underline{\xi})}}. \tag{A13}$$

Herein a second set of McCauley brackets is used to describe the actual stress state, which can lie far beyond the yield surface

$$\ll Y \gg = \begin{cases} Y, & \text{if } F > 0 \text{ and } LC > 0 \\ 0, & \text{else} \end{cases}. \tag{A14}$$

Introducing again the uniaxial form of the model with the so-called generalized overstress Λ (Bruhns, 1984; Bruhns and Rott, 1994)

$$\begin{aligned} \dot{\sigma} &= E \left(\dot{\varepsilon} - \sqrt{\frac{2}{3}} \Phi(\Lambda, T) \right) \\ \dot{\xi} &= c(\kappa, T) \sqrt{\frac{2}{3}} \Phi(\Lambda, T) \\ \dot{\kappa} &= \sqrt{\frac{3}{2} g(\kappa, T)} \sqrt{\frac{2}{3}} \Phi(\Lambda, T) \end{aligned} \tag{A15}$$

$$\Phi(\Lambda, T) = 2\gamma(T) \frac{\Lambda}{E(T)} \left(1 + \frac{\Lambda}{c_4(T)} \right)^{c_5(T)}$$

$$\Lambda = \sqrt{\left(\frac{2}{3} \sigma - \xi \right) \left(\sigma - \frac{3}{2} \xi \right)} - \sqrt{g(\kappa, T)}$$

one finds a certain disadvantage in the model; for vanishing overstresses the model becomes purely elastic. To overcome this situation, certain improvements are shown in Bruhns and Rott (1994) and Westerhoff (1995). The basic idea is to split the inelastic strain rate in two parts; the first describes the rate-independent hardening effects, the second contains all viscous effects

$$\dot{\underline{\epsilon}} = \dot{\underline{\epsilon}}_r + \dot{\underline{\epsilon}}_i = \dot{\underline{\epsilon}}_r + \dot{\underline{\epsilon}}_p + \dot{\underline{\epsilon}}_v. \tag{A16}$$

For the viscous strain rate, the above proposed concept of overstresses remains valid. A difference to the former formulation of the model occurs now for vanishing overstresses; in this case the extended model still contains plastic flow

$$\dot{\underline{\sigma}}_p = \frac{\dot{\underline{\sigma}} : \frac{\underline{\sigma}' - \underline{\xi}}{\sqrt{(\underline{\sigma}' - \underline{\xi}) : (\underline{\sigma}' - \underline{\xi})}}}{\frac{\frac{2}{3} E_t}{1 - \frac{E_t}{E}}} \frac{\underline{\sigma}' - \underline{\xi}}{\sqrt{(\underline{\sigma}' - \underline{\xi}) : (\underline{\sigma}' - \underline{\xi})}}. \tag{A17}$$

This formulation of the flow rule requires an additional evolution equation for the associated static stresses, i.e. the stresses on the yield surface. In Bruhns and Rott (1994) the following equation is introduced

$$\dot{\underline{\sigma}}' = \langle AC\Lambda, v, T \rangle \underline{\sigma}' + B(\underline{\sigma}', \underline{\xi}, T)(\underline{\sigma}' - \underline{\sigma}'). \tag{A18}$$

It should be stated here that in this model the stress on the yield surface is not time independent, e.g. it is increasing during creep processes due to the increasing inelastic work. For further details see Bruhns and Rott (1994). Eq. (A18) contains two additional material functions. The first one, $A(\Lambda, v, T)$, determines the evolution of the static stresses. In the case of vanishing overstresses the quantity v , which stands for the velocity of the process, still enables the model to describe hardening effects. In this paper we chose the Euclidean norm of the stress rate as a measure of the process velocity

$$v = \|\dot{\underline{\sigma}}'\|_2 := \sqrt{\sum_{i,k=1}^3 |\dot{\sigma}'_{ik}|^2}. \tag{A19}$$

The material function A is given in Bruhns and Rott (1994) as

$$A(\Lambda, \nu, T) = a_1(\Lambda, T)a_2(\nu, T) \tag{A20}$$

wherein

$$a_1(\Lambda, T) = \frac{1 - a_{11}(T)}{\tanh(a_{13}(T)) - 1} \left(\tanh(a_{12}(T) \frac{\Lambda}{\sigma_F} + a_{13}(T)) - 1 \right) + a_{11}(T) \tag{A21}$$

$$a_2(\nu, T) = a_{21}(T)e^{a_{22}(T)(\nu - \nu_0)^{a_{23}(T)}} + (1 - a_{21}(T))e^{a_{24}(T)(\nu - \nu_0)^{a_{25}(T)}}.$$

The second function $B(\underline{\sigma}', \underline{\xi}, T)$ was introduced to describe creep processes. Therefore the function depends on the stress level at the beginning of any creep process

$$B(\underline{\sigma}', \underline{\xi}, T) = d_3(\underline{\sigma}', T) \tanh(d_4(\underline{\sigma}', T) \sqrt{(\underline{\sigma}' - \underline{\xi}) : (\underline{\sigma}' - \underline{\xi})} / \sigma_F + d_5(\underline{\sigma}', T)) + d_6(\underline{\sigma}', T) \tag{A22}$$

with

$$\begin{aligned} d_3 &= p_{31} + p_{32} \|\underline{\sigma}'\|_2 / \sigma_F + p_{33} (\|\underline{\sigma}'\|_2 / \sigma_F)^2 \\ d_4 &= p_{41} + p_{42} \|\underline{\sigma}'\|_2 / \sigma_F + p_{43} (\|\underline{\sigma}'\|_2 / \sigma_F)^2 \\ d_5 &= p_{51} + p_{52} \|\underline{\sigma}'\|_2 / \sigma_F + p_{53} (\|\underline{\sigma}'\|_2 / \sigma_F)^2 \\ d_6 &= p_{61} + p_{62} \|\underline{\sigma}'\|_2 / \sigma_F + p_{63} (\|\underline{\sigma}'\|_2 / \sigma_F)^2. \end{aligned} \tag{A23}$$

Introducing again the uniaxial form of the model one gets the following equations:

$$\begin{aligned} \dot{\sigma} &= \frac{E}{1 + \left\langle \frac{A(\Lambda, \nu)(E - E_t(\kappa))}{E_t(\kappa)} \right\rangle} \left\{ \dot{\epsilon} - \ll \frac{B(\sigma, \xi) \left(1 - \frac{E_t(\kappa)}{E} \right)}{E_t(\kappa)} (\sigma - \dot{\sigma}) \gg \right. \\ &\quad \left. - \sqrt{\frac{2}{3}} \ll \Phi(\Lambda) \gg \operatorname{sign} \left(\frac{2}{3} \bar{\sigma} - \xi \right) \right\}, \quad \dot{\xi} = c(\kappa) \left(1 - \frac{E_t(\kappa)}{E} \right) \frac{\dot{\bar{\sigma}}}{E_t(\kappa)} \\ \dot{\kappa} &= \sqrt{\frac{3}{2}} g(\kappa) \left(1 - \frac{E_t(\kappa)}{E} \right) \frac{\dot{\bar{\sigma}}}{E_t(\kappa)} \quad \dot{\bar{\sigma}} = \langle A(\Lambda, \nu) \dot{\sigma} \rangle + \ll B(\sigma, \xi) (\sigma - \bar{\sigma}) \gg \end{aligned} \tag{A24}$$

The model in the form (A24) contains 22 parameters together with the parameters of the underlying static theory as given Section 4. The values for these parameters at room temperature are as follows:

$$a_{11} = 171 \quad a_{12} = 10.176 \quad a_{13} = -0.26 \\ a_{21} = 0.032 \quad a_{22} = -2.14 \quad a_{23} = 0.05 \quad a_{24} = -6.16 \quad a_{25} = 0.004$$

$$d_1 = 8.0 \times 10^{-12} \quad d_2 = 5.01$$

$$p_{31} = 2.0 \times 10^{-9} \quad p_{32} = 5.25 \times 10^{-7} \quad p_{33} = 9.61 \times 10^{-10} \quad [s^{-1}] \\ p_{41} = 23.85 \quad p_{42} = 1.125 \quad p_{43} = 1.704 \quad [-] \\ p_{51} = -14.57 \quad p_{52} = -34.98 \quad p_{53} = -0.784 \quad [-] \\ p_{61} = 0.00032 \quad p_{62} = 7.79 \times 10^{-9} \quad p_{63} = 1.09 \times 10^{-8} \quad [s^{-1}].$$

References

- Adelmann, H.M., Haftka, R., 1986. Sensitivity analysis of discrete structural systems. *AIAA Journal* 24, 823–832.
- Anding, D.K., 1997. Zur simultanen Bestimmung materialabhängiger Koeffizienten inelastischer Stoffgesetze. Ph.D. dissertation, Mitteilungen aus dem Institut für Mechanik 109, Ruhr-Universität Bochum.
- Andresen, K. et al., 1996. Parameteridentifikation für ein plastisches Stoffgesetz mit FE-Methoden und Rasterverfahren. *Bauingenieur* 71, 21–31.
- Banks, H.T., Kunisch, K., 1989. Estimation techniques for distributed parameter systems. Birkhäuser, Boston.
- Bard, Y., 1974. Nonlinear parameter estimation. Academic Press, New York.
- Baumeister, J., 1987. Stable solution of inverse problems. Vieweg, Braunschweig.
- Bodner, S.R., Partom, Y., 1975. Constitutive equations for elastic viscoplastic strain hardening materials. *Trans. ASME, J. Appl. Mech.* 42, 385–389.
- Braasch, H., Duddeck, H., Ahrens, H., 1995. New approach to improve material models. *Trans. ASME, J. Engng. Mat. Technol.* 117, 14–19.
- Braess, D., 1997. Finite elements. Cambridge University Press, Cambridge.
- Bruhns, O.T., 1984. The INTERATOM (IA) model. In: Bruhns, O.T. (Ed.), *Constitutive Modelling in the Range of Inelastic Deformations — A State of the Arts Report, INTERATOM*, pp. 33–63.
- Bruhns, O.T., Pitzer, M., 1987. Constitutive modelling in the range of inelastic deformations — evaluation of parameters. In: White, P. (Ed.), *Constitutive Modelling in the Range of Inelastic Deformations — Uniaxial Evaluations (GEC Report)*. GEC Research Ltd.
- Bruhns, O.T., Rott, U., 1994. A viscoplastic model with a smooth transition to describe rate-independent plasticity. *Int. J. Plasticity* 10, 347–362.
- Bui, H.D., 1994. Inverse problems in the mechanics of materials, an introduction. CRC Press, Boca Raton, London.
- Bui, H.D., Tanaka, M. et al. (Eds.), 1994. *Inverse Problems in Engineering Mechanics*, A.A. Balkema, Rotterdam.
- Cailletaud, G., Pilvin, P., 1993. Identification and Inverse Problems: A Modular Approach. ASME.
- Chaboche, J.-L., 1989. Constitutive equations for cyclic plasticity and cyclic viscoplasticity. *Int. J. Plasticity* 5, 247–302.
- Chaboche, J.-L., Rousselier, G., 1983. On the plastic and viscoplastic constitutive equations — part I: rules developed with internal variable concept. *Trans. ASME, J. Pressure Vessel Technol.* 105, 153–158.
- Collatz, L., Wetherling, W., 1966. Optimierungsaufgaben. Springer-Verlag, Berlin, Heidelberg, New York.
- Cordts, D., Kollmann, F.G., 1986. An implicit time integration scheme for inelastic constitutive equations with internal state variables. *Int. J. Num. Methods Eng.* 23, 533–554.
- Dennis, J.E., Schnabel, R.B., 1983. Numerical methods for unconstrained optimization and nonlinear equations. Prentice-Hall, Englewood Cliffs, NJ.

- Eftis, J., Abdel-Kader, M.S., Jones, D.L., 1989. Comparisons between the modified Chaboche and Bodner-Partom viscoplastic constitutive theories at high temperature. *Int. J. Plasticity* 5, 1–27.
- Furukawa, T., Yagawa, G., 1997. Inelastic constitutive parameter identification using an evolutionary algorithm with continuous individuals. *Int. J. Num. Meth. Eng.* 40, 1071–1090.
- Gavrus, A., Massoni, E., Chenot, J.L., 1994. Computer aided rheology for nonlinear large strain thermoviscoplastic behaviour formulated as an inverse problem. In: Bui, H.D. (Ed.), *Inverse Problems in Engineering Mechanics*. A.A. Balkema, Rotterdam, pp. 123–130.
- Geist, A. et al., 1994. PVM: Parallel virtual machine, a user's guide and tutorial for networked parallel computing. The MIT Press, Cambridge, MA.
- Gelin, J.C., Ghouati, O., 1996. An inverse solution procedure for material parameter identification in large plastic deformations. *Comm. Num. Meth. Eng.* 12, 161–173.
- Gerdes, R., Thielecke, F., 1996. Micromechanical development and identification of a stochastic constitutive model. *ZAMM* 76, S4:587–590.
- Großmann, Ch., Terno, J., 1993. *Numerik der Optimierung*. Teubner Studienbücher, Stuttgart.
- Hartmann, G., Kollmann, F.G., 1987. A computational comparison of the inelastic constitutive models of Hart and Miller. *Acta Mechanica* 69, 139–165.
- Heinhold, J., Gaede, K.-W., 1972. *Ingenieur-Statistik*. R. Oldenbourg Verlag, München, Wien.
- Khan, A.S., Huang, S., 1995. *Continuum theory of plasticity*. John Wiley & Sons, New York.
- Kreißig, R., 1996. Parameteridentifikation inelastischer Deformationsgesetze. *Techn. Mechanik* 16, 97–106.
- Krempf, E., 1987. Models of viscoplasticity. Some comments on equilibrium (back) stress and drag stress. *Acta Mechanica* 69, 25–42.
- Krempf, E., Lu, H., 1984. The hardening and rate-dependent behavior of fully annealed AISI type 304 stainless steel under biaxial in-phase and out-of-phase strain cycling at room temperature. *Trans ASME, J. Engng. Mat. Technol.* 106, 376–382.
- Kublik, F., Steck, E., 1992. Comparison of two constitutive models with one- and multiaxial experiments. In: Besdo, D. & Stein, E. (Eds.). *Finite Inelastic Deformations — Theory and Applications*. IUTAM Symposium, Hannover, 1991. Springer-Verlag, Berlin, pp. 37–46.
- Kunkel, R., Kollmann, F.G., 1997. Identification of constants of a viscoplastic constitutive model for a single crystal alloy. *Acta Mechanica* 124, 27–45.
- Lambert, J.D., 1983. *Computational methods in ordinary differential equations*. John Wiley & Sons, New York.
- Lehmann, Th., 1989. On the balance of energy and entropy at inelastic deformations of solid bodies. *Eur. J. Mech., A/Solids* 8, 235–251.
- Lemaitre, J., Chaboche, J.-L., 1990. *Mechanics of solid materials*. Cambridge University Press, Cambridge.
- Louis, A.K., 1989. *Inverse und schlecht gestellte Probleme*. Teubner, Stuttgart.
- Mahnken, R., Stein, E., 1989. Adaptive time-step control in creep analysis. *Int. J. Num. Meth. Eng.* 28, 1619–1633.
- Mahnken, R., Stein, E., 1994a. Gradient-based methods for parameter identification of viscoplastic materials. In: Bui, H.D. et al. (Eds.), *Inverse problems in engineering mechanics*. A.A. Balkema, Rotterdam, pp. 137–144.
- Mahnken, R., Stein, E., 1994b. The identification of parameters for visco-plastic models via finite-element-methods and gradient-methods. *Modelling Simul. Mater. Sci. Eng.* 2, 597–616.
- Mahnken, R., Stein, E., 1996a. Parameter identification for viscoplastic models based on analytical derivatives of a least-squares functional and stability investigations. *Int. J. Plasticity* 12, 451–479.
- Mahnken, R., Stein, E., 1996b. A unified approach for parameter identification of inelastic material models in the frame of finite element method. *Comp. Meth. Appl. Mech. Eng.* 136, 225–258.
- Mahnken, R., Stein, E., 1997. Parameter identification for finite deformation elasto-plasticity in principal direction. *Comp. Meth. Appl. Mech. Eng.* 147, 17–39.
- Miller, A.K., 1987. *Unified constitutive equations for creep and plasticity*. Elsevier Applied Science, London, New York.
- Morozov, V.A., 1984. *Methods for solving incorrectly posed problems*. Springer-Verlag, New York.

- Müller, D., Hartmann, G., 1989. Identification of material parameters for inelastic constitutive models using principles of biologic evolution. *Trans. ASME, J. Engng. Mat. Technol.* 111, 299–305.
- Nouailhas, D., 1989. Unified modelling of cyclic viscoplasticity: application to austenitic stainless steel. *Int. J. Plasticity* 5, 501–520.
- Ohtani, R., Ohnami, M., Inoue, T., 1988. *High temperature creep-fatigue*. Elsevier Applied Science, London, New York.
- Ostermeier, A., Gawelczyk, A., Hansen, N., 1994. Step-size adaptation based on a non-local use of selection information. In: Davidor, Y., Schwefel, H.-P., Männer, R. (Eds.), *Proceedings of the Third Conference on Parallel Problem Solving from Nature — PPSN III*, Jerusalem. Springer-Verlag, pp. 189–198.
- Perzyna, P., 1977. Fundamental problems of viscoplasticity. In: Yih, C.S. (Ed.), *Advances in Applied Mechanics*, Vol. 9, ed.. Academic Press, New York, pp. 243–377.
- Press, W.H., 1992. *Numerical Recipes in FORTRAN: The Art of Scientific Computing*. Cambridge University Press, Cambridge.
- Rechenberg, I., 1973. *Evolutionsstrategie*. Frommann-Holzboog, Stuttgart.
- Rentrop, P., Strehmel, K., Weiner, R., 1966. Ein Überblick über Einschrittverfahren zur numerischen Integration in der technischen Simulation. *GAMM-Mitteilungen* 19, 9–43.
- Schinke, B., Schwertel, J., 1994. Bestimmung der Parameter viskoplastischer Werkstoffmodelle. *ZAMM* 74, 233–235.
- Schittkowski, K., 1981. The nonlinear programming method of Wilson, Han and Powell with an augmented Lagrangian type line search function. *Numerische Mathematik* 38, 83–114.
- Schlums, H., Steck, E.A., 1992. Description of cyclic deformation process with a stochastic model for inelastic behaviour of metals. *Int. J. Plasticity* 8, 147–159.
- Schöneburg, E., Heinzmann, F., Feddersen, S., 1994. *Genetische Algorithmen und Evolutionsstrategien: Eine Einführung in Theorie und Praxis der simulierten Evolution*. Addison-Wesley, Bonn, Paris.
- Schwefel, H.-P., Hammel, U., Bäck, T., 1994. Evolutionäre Algorithmen: optimieren nach dem Vorbild der biologischen evolution. *Der GMD-Spiegel* 2, 49–58.
- Senseny, P.E., Brodsky, N.S., DeVries, K.L., 1993. Parameter evaluation for a unified constitutive model. *Trans. ASME, J. Engng. Mat. Technol.* 115, 157–162.
- Stein, E., Wriggers, P., 1989. *Computational mechanics bei Festkörpern und Ingenieursstrukturen unter Verwendung von Finite-Element-Methoden*. *GAMM-Mitteilungen* 1, 3–39.
- Tarantola, A., 1987. *Inverse problem theory, methods for data fitting and model parameter estimation*. Elsevier, Amsterdam, Oxford, New York.
- Westerhoff, B., 1995. *Eine Untersuchung zum geschwindigkeitsabhängigen Verhalten von Stahl*. Ph.D. dissertation, *Mitteilungen aus dem Institut für Mechanik 99*, Ruhr-Universität Bochum.
- White, C.S., Bronkhorst, C.A., Anand, L., 1990. An improved isotropic-kinematic hardening model for moderate deformation metal plasticity. *Mech. Materials* 10, 127–147.